QRPA treatment of the transverse wobbling mode reconsidered

S. Frauendorf[1,*] and F. Dönau†

[1] *Department of Physics, University of Notre Dame, South Bend, Indiana 46556*

Abstract

The quasiparticle random phase approximation is used to study the properties of the wobbling bands in ^{163}Lu. Assuming that the wobbling mode represents pure isoscalar orientation oscillations results in too low wobbling frequencies and too strong M1 transitions between the one- and zero-phonon wobbling bands. The inclusion of an LL interaction, which couples the wobbling mode to the scissors mode, generates the right upshift of the wobbling frequencies and the right suppression of the B(M1)$_{out}$ values toward the experimental values. In analogy to the quenching of low-energy E1 transition by coupling to the Isovector Giant Dipole Resonance, a general reduction of the M1 transitions between quasiparticle configurations caused by coupling to the scissors mode is suggested.

PACS numbers: 21.10.Re, 23.20.Lv, 27.70.+q

arXiv:1509.08116v1 [nucl-th] 27 Sep 2015

I. INTRODUCTION

Rotating nuclei that have a triaxially deformed shape are expected exhibit a characteristic excitation mode called "wobbling" by Bohr and Mottelson [1], which is an orientation vibration of the triaxial body about the rotational axis. It is the nuclear analog to the motion of the classical top with three different moments of inertia, which is well known from the rotational spectra of molecules. Experimental evidence for the wobbling mode was established by the discovery [2–4] of rotational bands in the ^{71}Lu isotopes when they attain a triaxial strongly deformed (TSD) shape at high spin. The simple dynamics of a rotor with three different moments of inertia results in an increase of the wobbling frequency with angular momentum, which is seen in molecules. However, for the Lu isotopes a decrease is observed, which makes the identification of the wobbling possible, because it prevents the mode being fragmented among competing quasiparticle excitations. In the framework of the Quasiparticle+Triaxial-Rotor (QTR) model, Frauendorf and Dönau [5] demonstrated that the decrease results from the presence of the odd $i_{13/2}$ quasi proton, which aligns its angular momentum along the short body axis, *transverse* to the medium axis with the largest moment of inertia. To notify the modification of the dynamics by the odd quasiparticle, they introduced the name "transverse wobbling". They predicted the appearance of transverse wobbling for the mass 130 region, where the $h_{11/2}$ quasiparticle couples transverse to the triaxial rotor. The prediction was recently confirmed for ^{135}Pr [6]. The QTR calculations well account for the wobbling energies and the B(E2)$_{con}$ values of the $\Delta I = 1$ electric quadrupole transitions, which connect the one-phonon wobbling band with the zero-phonon band. However, the B(M1)$_{con}$ values of the connecting magnetic dipole transitions are overestimated by about a factor of 3-10 (see Ref. [6] and Ref. [5]). The discrepancy turns out to be robust, and it can be traced back to the transverse geometry: For a quasiproton that is rigidly coupled to the triaxial charge density distribution (HFA approximation of Ref. [5]) the amplitude of the wobbling vibrations of the charge density, which generate the B(E2)$_{out}$ values of the inter band transitions, determines the the amplitude of the vibrations of the magnetic moment of the odd quasi proton, which generate the B(M1) values of the inter band transitions. Realistically, the odd quasi proton is not rigidly coupled to the rotor, which reduces the amplitude of the oscillations of the magnetic moment and thus the B(M1)$_{out}$ values. However the reduction is too weak to bring down the B(M1)$_{out}$ to the experimental values (see Fig. 19 of Ref. [5]). The present paper addresses this problem of the too strong magnetic dipole transitions from a microscopic perspective.

Following the discovery of the first wobbling structure in ^{163}Lu [2], Hamamoto, Hagemann *et al.* [2, 7, 8] used the QTR model to describe the wobbling mode. These calculations made the ad hoc assumption that the short axis has the largest moment of inertia, by exchanging the hydrodynamic moments of inertia of the short and medium axes. The large ratios B(E2)$_{out}$/B(E2)$_{in}$ of inter-band to intra-band E2 transitions could be well reproduced. The B(M1)$_{out}$ were only overestimated by a factor of 2-3. However, the calculated wobbling frequencies of the QTR model with the "inverted moments of inertia" assumption distinctly disagree with experiment. Instead of the experimentally observed decrease, the wobbling frequency increases with the spin I, which is expected because the inverted moment of inertia arrangement corresponds to the longitudinal wobbling geometry in the terminology of Ref. [5]. Ref. [9] suggested to remedy the problem by assuming a decrease of the scale of the rotational energy, which may reflect the increase of the moments of inertia due to a reduction of the pair correlations. In our view, the "inverted moments of inertia" assumption is unrealistic because any microscopic calculation of the three moments of inertia in the frame of the cranking model give the maximal moment of inertia for the medium axis. This result is in accordance with

*Electronic address: sfrauend@nd.edu

the hydrodynamic ratios between the moments of inertia. It can be qualitatively understood by the fact that the moment of inertia of a certain axis increases with the deviation from cylindric symmetry, which is maximal for the medium axis. Hence, the problem with the too strong magnetic transition remains.

The observation of the wobbling mode stimulated theoretical efforts to understand how the nuclear shell structure and the residual interaction generate such a type of collective excitations. Matsuyanagi, Matsuzaki, Ohtsubo, Shimizu, and Shoji demonstrated that the quasiparticle random phase approximation (QRPA) is an adequate microscopic approach [10–14]. QRPA describes wobbling bands in terms of correlated two-quasiparticle excitations in a rotating triaxial potential. Relevant results of these studies can be summarized as follows.
- The QRPA calculations agree with the transverse wobbling geometry as discussed in Ref. [5]. The authors refers to it as "positive γ shape", which uses the common terminology of principle axis cranking that assigns the sector $0 \leq \gamma \leq 60^\circ$ to rotation about the short axis. The angular momentum of the odd $i_{13/2}$ quasiparticle aligns with this axis. The decrease of the wobbling frequency is interpreted as the approach of the instability of the cranking solution to a tilt of the rotational axis into the short-medium plane, which is signaled by the frequency of the lowest QRPA solution to become zero [12].
-The collective enhancement of the connecting E2 transitions is born out. QRPA calculations based on the Niisson potential underestimate the ratios $B(E2)_{out}/B(E2)_{in}$ by about a factor of two [10–12], the ones based on a Woods-Saxon potential get it right [13].
-The $B(M1)_{out}$ values of the inter band transitions are overestimated by a factor of 10 as for the QTR results for transverse wobbling.

The QRPA calculations [10–12] used an isoscalar quadrupole-quadrupole (QQ) residual interaction. Because such interaction generates the same coupling between the odd quasiparticle and the triaxial rotor core as in the QTR calculations, it comes as no surprise that both approaches overestimate $B(M1)_{out}$ values by the same factor. The reason to revisit the QRPA in this paper is to investigate how modifying the residual interaction influences the resulting excitation energies and electromagnetic transition rates. In particular we are interested whether the suppression of the inter band M1 transitions can be obtained for transverse wobbling. We study the $i_{13/2}$ TSD bands in ^{163}Lu which offer the most complete set of data.

The paper is organized as follows. In Sec.II A a selfconsistent treatment of the QRPA is performed by deriving the shape parameters (ε, γ) from the QQ interaction. In Sec.II B the shape parameters (ε, γ) are adopted from a Nilsson-Strutinsky minimization [17] and the strength of residual QQ interaction is determined by restoring the rotational invariance of the Hamiltonian. Sec.III studies the consequences of additional interactions. Coupling to the low-energy orbital M1 resonance ("scissors mode") is suggested as a mechanism that suppresses the strength of the M1 inter band transitions. Sec. IV summarizes the results and puts them into perspective.

II. QUASIPARTICLE RANDOM PHASE APPROXIMATION (QRPA) FOR ISOSCALAR QQ INTERACTION

A. Selfconsistent QRPA (sc QRPA) with standard QQ interaction

The theoretical framework of our QRPA calculations is similar to the one used in our recent study of chiral vibrations [15]. The Hamiltonian $\hat{H}'$ is defined with respect to a reference system rotating about the 1-axis,

$$\hat{H}' = \hat{H} - \omega \hat{J}_1, \tag{1}$$

where ω is the cranking frequency and $\hat{J}_1$ denotes the 1-component of the angular momentum operator. The cranking term $-\omega \hat{J}_1$ ensures that the states have an average angular momentum $\langle J_1 \rangle = I$. The corresponding lab. Hamiltonian $\hat{H}$ in Eq.(1) is

$$\begin{aligned} \hat{H} \;=\; & \sum_{\tau=\pi,\nu} [\; \hat{h}^\circ_\tau - \Delta_\tau(\hat{P}^\dagger_\tau + \hat{P}_\tau) - \lambda_\tau \hat{N}_\tau \;] \\ & - \frac{\kappa_0}{2} \sum_{m=-2,2} (-1)^m \hat{Q}_m \hat{Q}_{-m}. \end{aligned} \tag{2}$$

The operator $\hat{h}^\circ_\tau$ is the spherical part of the Nilsson Hamiltonian where the isospin index $\tau = \pi, \nu$ distinguishes the neutron and proton contributions, respectively. The term $\Delta_\tau(\hat{P}^\dagger_\tau + \hat{P}_\tau)$ accounts for the pair field where $\hat{P}^\dagger_\tau$ and $\hat{P}_\tau$ are the familiar monopole pair operators. Aiming at the high-spin $\pi i_{13/2}$ band in ^{163}Lu, the gap parameters Δ_τ are assumed to be reduced: below the cranking frequency ω=0.45 MeV we take Δ_π=0.45 MeV for the proton gap and Δ_ν=0.35 MeV for the neutron gap, and we use $\Delta_{\tau=\pi,\nu}$=0 above. As usual, the terms $\lambda_\tau \hat{N}_\tau$, containing the particle number operators $\hat{N}_\tau$, are introduced to attain the average particle numbers $\langle \hat{N}_\pi \rangle = Z$ and $\langle \hat{N}_\nu \rangle = N$, respectively, by an appropriate choice of the Fermi energy λ_τ. The following term in Eq. (2) is the isoscalar quadrupole-quadrupole (ISQQ) interaction constructed from the mass quadrupole operators $\hat{Q}_m = \hat{Q}_m(\pi) + \hat{Q}_m(\nu)$ where $\hat{Q}_m(\tau) \equiv \sqrt{4\pi/5}\,(r/b_\circ)^2 Y_{2m}(\tau)$ and $b_\circ = 1.01A^{1/3}$ is the oscillator length.

In this section we assume selfconsistency between the ISQQ interaction and the deformed nuclear shape defined by the parameters (ε, γ). More precisely, it is the deformed mean field potential v of the ISQQ interaction which, for a predefined interaction strength κ_0, has to obey the condition

$$v = v(\varepsilon, \gamma) = -\kappa_0 [\langle \hat{Q}_0 \rangle \hat{Q}_0 + \langle \hat{Q}_2 \rangle (\hat{Q}_2 + \hat{Q}_{-2})], \tag{3}$$

TABLE I: Equilibrium values of the deformation parameters (ε, γ) in the frequency region ω = 0.15-0.50 MeV/$\hbar$. The strength parameter of the ISQQ interaction is κ_0= 0.01960 MeV

ω(MeV/$\hbar$)	ε	γ(deg)
0.15	0.398839	9.248
0.20	0.397926	9.362
0.25	0.396632	9.486
0.30	0.394788	9.631
0.35	0.392064	9.798
0.40	0.387658	9.977
0.45	0.381236	11.575
0.50	0.377065	11.619

where $|\rangle = |\varepsilon, \gamma\rangle$ is the quasiparticle reference state of the $\pi i_{13/2}$ TSD band as specified below. Denoting the c-numbers $\langle \hat{Q}_{0,2} \rangle$ as $q_{0,2}(\varepsilon, \gamma)$ the selfconsistency conditions demand searching for deformation parameters which at a given cranking frequency ω satisfy the relations

$$\begin{aligned} \kappa_0 \langle \hat{Q}_0 \rangle \equiv \kappa_0 q_0(\varepsilon, \gamma) &= 2/3\, \hbar\omega_0\, \varepsilon \cos\gamma, \\ \kappa_0 \langle \hat{Q}_2 \rangle \equiv \kappa_0 q_2(\varepsilon, \gamma) &= -2/3\, \hbar\omega_0\, \varepsilon \sin\gamma/\sqrt{2}. \end{aligned} \quad (4)$$

The mean field calculations are done by using the tilted axis cranking (TAC) code described in Ref. [16]. It should be noted that the above conditions lead to a stable equilibrium shape only if one renders the volume conservation by taking the scale factor $\hbar\omega_0 = 41 A^{-1/3}$ MeV as constant. Combining the spherical mean field part from the Hamiltonian $\hat{H}'$, Eq.(1), with the selfconsistency conditions (4), one obtains the mean field Hamiltonian of the 1D-TAC model $\hat{h}' = \hat{h} - \omega \hat{J}_1$ [16], where $\hat{h}$ is given by

$$\begin{aligned} \hat{h} = \hat{h}^\circ - \Delta_\tau (\hat{P}^\dagger + \hat{P}) - \lambda \hat{N} - \\ - \hbar\omega_0 \frac{2}{3} \varepsilon \left(\cos\gamma \hat{Q}_0 - \frac{\sin\gamma}{\sqrt{2}} (\hat{Q}_2 + \hat{Q}_{-2}) \right). \end{aligned} \quad (5)$$

The diagonalization of the TAC Hamiltonian $\hat{h}$ is done in an oscillator basis with the quantum numbers $\{n, l, j, m\}$ including the orbits of the three main shells $n = 4 - 6$. The search for the equilibrium needs to be performed with diabatic tracing (c.f. [16]) of the selected $(\pi i_{13/2}, \nu$ g) configuration of the TSD band. The strength of the sc ISQQ interaction κ_0= 0.01960 MeV is ω-independent and chosen such that at $\omega = 0.15$ MeV/$\hbar$ the deformation parameter comes close to the suggested value $\varepsilon = 0.4$ of the experimental TSD band [17]. The sc deformation parameters for the frequency interval ω=0.15-0.50 MeV/$\hbar$ are presented in Table I. It is seen that for the ISQQ interaction the sc triaxiality parameter $\gamma \approx 9 - 12°$ is lower than $+20°$ suggested in Ref. [17], but close to the values found by Shoji and Shimizu [13] with Nilsson-Strutinsky minimization. The relative change of the deformation (ε, γ) to higher rotational frequencies is small. Nevertheless precise selfconsistency is required in the subsequent

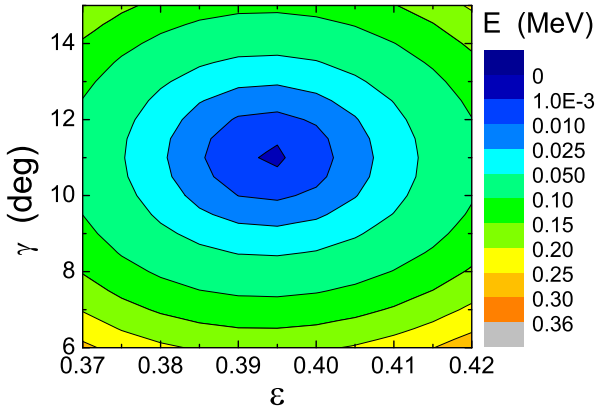

FIG. 1: (Color online) Total routhian surface for the TSD configuration in ^{163}Lu at $\omega = 0.45$ MeV/$\hbar$.

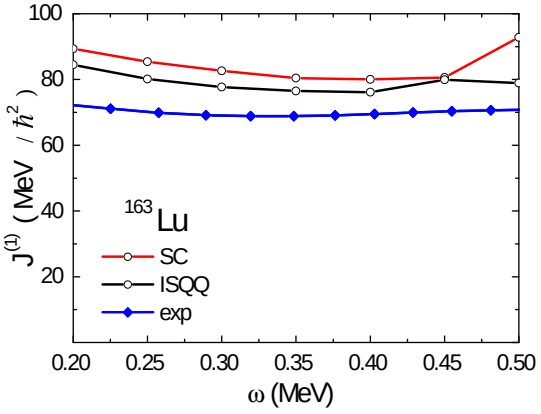

FIG. 2: (Color online) Experimental and calculated kinematic moments of inertia of the TSD band in ^{163}Lu. The calculated moment of inertia is $\mathcal{J}^{(1)} = \langle J_1 \rangle / \omega$.

QRPA calculation in order to obtain reliable values for the excitation energies and E2/M1 properties of the wobbling band. As already noted in the previous QRPA papers [10–14], the absolute minimum of $\langle \hat{H}' \rangle$ corresponds to rotation about the short axis of the triaxial potential, along which the angular momentum of the $i_{13/2}$ proton is aligned (the sector of positive γ-values in standard Principle Axis Cranking (PAC) terminology). Above the frequency ω=0.5 MeV/$\hbar$ the PAC solution becomes unstable, because the moment of inertia of the medium axis is larger than the one of the short axis. The stable solution corresponds to rotation about a *tilted* axis in the short-medium plane, which represents a $\Delta I = 1$ band. The QRPA frequency goes to zero when approaching the instability from below. Thus, the QRPA solution studied in this paper is of the "transverse wobbling" type according to the classification scheme introduced by us in Ref. [5], where the corresponding physics is discussed in the

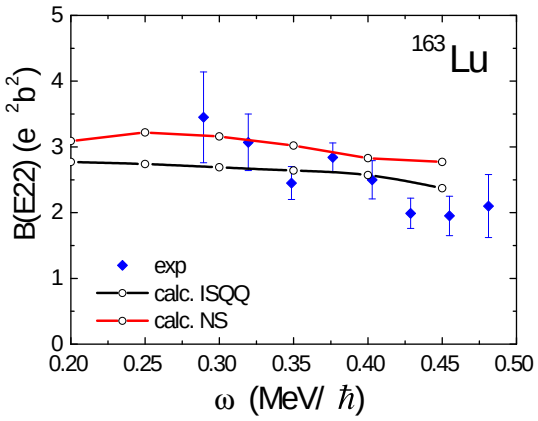

FIG. 3: (Color online) Experimental and calculated B(E2,I→I-2) values of the TSD band.

semiclassical frame work of the HFA approximation.

In Fig. 1 we show the total routhian surface for ω=0.45 MeV/$\hbar$ as obtained by diabatic tracing the TSD configuration with the TAC code. The ISQQ interaction gives a relatively shallow minimum on the deformation surface. In Fig. 2 the experimental and calculated moments of inertia $\mathcal{J}^{(1)}$ are compared. The experimental frequencies of the TSD bands are derived by using the standard definition $\omega(\bar{I}) = (E(I) - E(I-2))/2$, where transition spin $\bar{I} = I - 1/2$, and the experimental moment of inertia $\mathcal{J}^{(1)}(\bar{I}) = \bar{I}//\omega(\bar{I})$. The calculation somewhat overestimates the experimental values.

Fig. 3 presents the experimental B(E2) values of the $I \rightarrow I-2$ transitions within the TSD g-band [17] and the ones calculated with the sc TAC model. The polarization charges e_p=(1+Z/A)e and e_n=Z/A e were adopted for the proton and neutron parts of the electric quadrupole operator.

Starting from results of the sc TAC calculation the QRPA is performed following the general formalism as outlined in the textbooks (e.g. [18]). We mention only the important steps of the QRPA and refer for more details to our recent paper [15]. Firstly, the Hamiltonian (1) is rewritten in quasiparticle (qp) representation,

$$\hat{H}' = \hat{h}' + \hat{V}_{4qp}, \tag{6}$$

where $\hat{h}'$ is the diagonalized TAC Hamiltonian

$$\hat{h}' = E_\circ + \sum_i e_i \hat{\alpha}_i^\dagger \hat{\alpha}_i. \tag{7}$$

The set $\{\hat{\alpha}_i^\dagger, \hat{\alpha}_i\}$ denotes the qp operators, e_i are the qp energies and $\hat{V}_{4qp}$ contains the residual 4qp interaction terms which give rise to the vibrational excitations. Then, the quasi-boson approximation $\hat{\alpha}_i^\dagger \hat{\alpha}_j^\dagger \Rightarrow \hat{b}_{ij}^\dagger$ is applied such that the Hamiltonian, Eq. (6), is expressed in terms of bosons, $\hat{H}' \Rightarrow \hat{H}'_{RPA}$, keeping only boson terms up to second order [18]. This Hamiltonian is diagonalized by using the QRPA equation

$$\left[\hat{H}'_{\rm QRPA},\ \hat{O}_\lambda^\dagger\right] = E^\lambda_{QRPA} \hat{O}_\lambda^\dagger, \tag{8}$$

which yields the phonon excitation energies E^λ_{QRPA} and the phonon excitation operators $\hat{O}_\lambda^\dagger$ defined by

$$\hat{O}_\lambda^\dagger = \sum_{\mu=i<j} (X^\lambda_\mu \hat{b}^\dagger_\mu - Y^\lambda_\mu \hat{b}_\mu). \tag{9}$$

The amplitudes X^λ_μ and Y^λ_μ are found by solving the standard set of linear equations following from Eq.(8). The quasiparticle Hamiltonian $\hat{h}'$ and the full Hamiltonian $\hat{H}'$ commute with the signature operator $R_1 = \exp(-i\pi \hat{I}_1)$, which generates a 180 deg rotation about the cranking axis. Therefore, the quasiparticle states and the phonon excitations have good signature quantum numbers. The energetically lowest phonon state with negative signature $r = -1$ embodies the wobbling excitation which is characterized also by giving the largest cross-over transition strength B(E2,$I \rightarrow I-1$). Accordingly, only 2qp components with the combined qp signature $r = r_i r_j = -1$ contribute to the wobbling operator $\hat{O}^\dagger$ in Eq.(9). One has to make sure that the spurious rotational solution with the energy $E_{QRPA} = \hbar\omega$ does not mix with the wobbling solution. Selfconsistency of the mean field ensures this requirement.

The E2/M1 transition amplitudes from the TSD wobbling band to the TSD g-band are obtained by evaluating the matrix element

$$\langle w|\hat{\mathcal{M}}_m(E2/M1)|0\rangle = \langle 0|\hat{O}_w \hat{\mathcal{M}}_m(E2/M1)|0\rangle, \tag{10}$$

where $|w\rangle$ means the wobbling phonon state and $|0\rangle$ denotes the QRPA vacuum state at the cranking frequency ω. The transition operators are

$$\begin{aligned} \hat{\mathcal{M}}_m(E2) &= e_p r_p^2 Y_{2m}(p) + e_n r_n^2 Y_m(n), \\ \hat{\mathcal{M}}_m(M1) &= \frac{3}{4\pi} g_p^{(l)} \hat{l}_{1m}(p) + g_p^{(s)} \hat{s}_{1m}(p) + g_n^{(s)} \hat{s}_{1m}(n). \end{aligned} \tag{11}$$

The component m is assigned to the transition $I \rightarrow I - m$. Further, the orbital g-factor for M1 is $g_p^{(l)} = 1\ \mu_N$ for protons and 0 for neutrons. The spin g-factors $g_p^{(s)}$ and $g_n^{(s)}$ are 0.7 times the values for the free proton or neutron. The reduced transition probabilities are

$$B(E2/M1, I \rightarrow I \mp 1) = \left|\left\langle w \left| \hat{\mathcal{M}}_{\pm 1}(E2/M1) \right| 0 \right\rangle\right|^2. \tag{12}$$

In the sc version of QRPA, the ISQQ term in the Hamiltonian (1) generates both the deformed mean field and the residual interaction. As discussed above, its strength is fixed to the value $\kappa_\circ = 0.01960$ for the whole frequency range ω =0.15-0.5 MeV/$\hbar$. The factorized form of the ISQQ term reduces the solution of the QRPA equation to searching the zeros of the dispersion determinant, which are located at the QRPA energies E_{QRPA}.

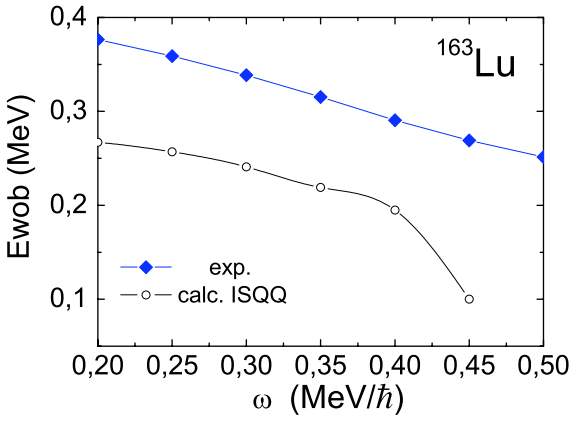

FIG. 4: (Color online) Excitation energy of the wobbling band in ^{163}Lu as a function of the rotational frequency. Experimental values (blue diamonds) are from [17]. QRPA calculation (solid line) with selfconsistent ISQQ interaction.

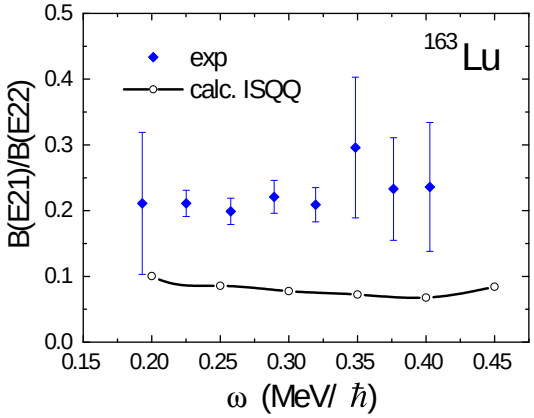

FIG. 5: (Color online) The ratios B(E21)/B(E22) between the inter and and intra band reduced transition probabilities B(E2, $I \to I-1)_{out}$/ B(E2, $I \to I-2)_{in}$ for the transitions between the TSD wobbling band and the TSD ground band in ^{163}Lu. Notations as in Fig. 4.

In Figs. (4 - 6) we present the QRPA results for the wobbling energies and the inter band B_{out}(E2, $I \to I-1$) and B_{out}(M1, $I \to I-1$) values. The reduced transition probabilities of the upward transitions $I \to I+1$ are at least one order smaller and not displayed. The calculated wobbling energies $E_{QRPA}(\omega)$ follow the decreasing tendency of the measured ones, which is characteristic for transverse wobbling. However, they are substantially below the experiment. At ω=0.45 MeV the frequency becomes zero, which signalizes the change to a permanent tilt of the rotational axis away from the short axis. The experimental wobbling energies decrease linearly up to ω=0.60 MeV. The calculated ratios between the inter and and intra band transition probabilities B(E2)$_{out}$/B(E2)$_{in}$ =B(E2, $I \to I-1$)/ B(E2, $I \to I-2$) reach only one half of the measured values, whereas the calculated B(M1, $I \to I-1$) exceed the experimental ones by a factor ten. Our results are similar to the ones of Ref. [11], who used the QRPA version for ISQQ interaction in the body fixed frame. The deviations from experiment are about the same.

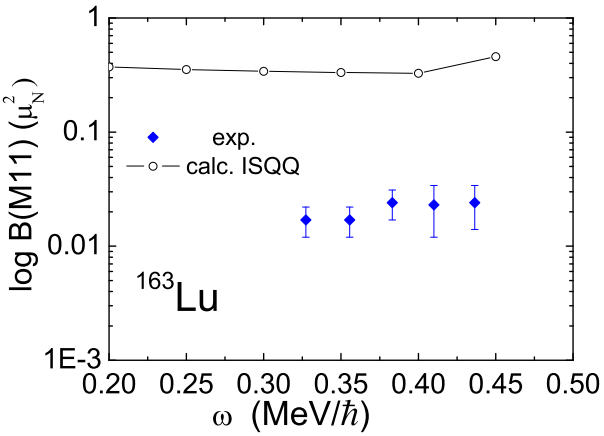

FIG. 6: (Color online) The reduced transition probabilities B(M11)= B(M1, $(I \to I-1))_{out}$ for the transitions between the TSD wobbling band to the TSD ground band in ^{163}Lu. Notations as in Fig. 4.

B. QRPA for freely chosen shape parameters

The wobbling mode is sensitive to the ratios between the three moments of inertia, which strongly change with the triaxality parameter γ. The ISQQ coupling constant $\kappa_\circ = 0.01960$ used in the preceding section was adjusted to obtain a mean field deformation of $\varepsilon = 0.4$. The sc values of $\gamma \approx 10^\circ$ obtained with the coupling constant fixed this way are substantially smaller than the values that are calculated by minimizing the Nilsson-Strutinsky energy functional, which are given in Tab. II. Ref. [14] demonstrated that larger values of γ increase the ratio $B(E2)_{out}/B(E2)_{in}$ between the inter and intra band transitions. Their QPPR version in the body fixed frame does not use the selfconsistency in an explicit way, allowing them to freely choose the deformation of the mean field. In order to investigate this possibility we need give up the selfconsistency requirement, Eq. (4), between the shape parameters and the QQ interaction in Eq. (2) with the common strength parameter κ_0. This means we use the same deformed mean field Hamiltonian $\hat{h}$, Eq. (5) as before but the values of (ε, γ) shall be at our disposal. Selfconsistency is only locally restored by constructing the residual interaction from the requirement that the resulting Hamiltonian $\hat{H} = \hat{h} + V_{4qp}$ becomes rotational

invariant. Such "symmetry-restoring interaction" [19, 20]

$$V_{4qp} = -\frac{1}{2}\sum_{m=1}^{3}\kappa_m F_m^2 \tag{13}$$

is built from the squares of the commutators of the quasiparticle Hamiltonian $\hat{h}$ and the angular momentum components $J_{m=1,2,3}$:

$$F_m = [\hat{h}, iJ_m]. \tag{14}$$

The strength constants κ_m are determined by demanding rotational invariance via the commutator

$$[\hat{H}, iJ_m] = [h - \frac{1}{2}\sum_{n=1}^{3}\kappa_n F_n^2, iJ_m] = 0 \tag{15}$$

which can be satisfied on average $\langle[\hat{H}, iJ_m]\rangle = 0$ by fixing the strength constants according to

$$\kappa_m^{-1} = \langle[[\hat{h}, iJ_m], iJ_m]\rangle \tag{16}$$

where $|\rangle$ is the reference quasiparticle configuration.

This method can be applied to any mean field Hamiltonian $\hat{h}$, as for instance in Ref. [13] to a deformed Woods-Saxon potential. In our case the commutator (14) with a quadrupole deformed field generates again quadrupole operators. Now we evaluate the commutators relations (14, 16) explicitly. The results are written in terms of the combined quadrupole operators $Q_{1\pm}$ and $Q_{2\pm}$ defined by

$$\begin{aligned} Q_{1+} &= \frac{Q_1 + Q_{-1}}{i\sqrt{2}}, \quad Q_{1-} = \frac{Q_1 - Q_{-1}}{\sqrt{2}}, \\ Q_{2+} &= \frac{Q_2 + Q_{-2}}{\sqrt{2}}, \quad Q_{2-} = \frac{Q_2 - Q_{-2}}{i\sqrt{2}}. \end{aligned} \tag{17}$$

Introducing for given deformations (ε, γ) the constants $\mathcal{Q}$ and $\tilde{\gamma}$ defined by

$$\begin{aligned} \mathcal{Q} &= \sqrt{\langle Q_0\rangle^2 + \langle Q_{2+}\rangle^2}\,, \\ \sin\tilde{\gamma} = -\frac{\langle Q_{2+}\rangle}{\mathcal{Q}}, &\qquad \cos\tilde{\gamma} = \frac{\langle Q_0\rangle}{\mathcal{Q}} \end{aligned} \tag{18}$$

the Hamiltonian (1) with the interaction (13) takes the form

$$\begin{aligned} \hat{H} = \hat{h} + \frac{1}{3}\frac{\hbar\omega_\circ\varepsilon}{\mathcal{Q}}\,[\,&\frac{\sin\gamma}{\sin\tilde{\gamma}}\,Q_{2-}^2 + \frac{\sin(\gamma+2\pi/3)}{\sin(\tilde{\gamma}+2\pi/3)}\,Q_{1+}^2 + \\ &+ \frac{\sin(\gamma-2\pi/3)}{\sin(\tilde{\gamma}-2\pi/3)}\,Q_{1-}^2\,] \end{aligned} \tag{19}$$

where the constants κ_m are expressed in terms of $\mathcal{Q}$ and $\tilde{\gamma}$. Hence, the residual interaction of the Hamiltonian $\hat{H}$, needed for the QRPA, is fully determined by the mean field part $\hat{h}$, in our case by its deformation parameters (ε, γ).

TABLE II: Deformation parameters (ε, γ) of ^{163}Lu in the frequency region ω = 0.15-0.55 MeV/$\hbar$ obtained from a Nilsson-Strutinsky (NS) minimization [17]

ω(MeV/$\hbar$)	ε	γ(deg)
0.15	0.3815	18.75
0.2	0.3892	19.2
0.25	0.3968	19.64
0.3	0.4044	20.12
0.35	0.408	20.41
0.4	0.3991	20.72
0.45	0.3908	21.3
0.5	0.3852	21.78
0.55	0.3812	22.34

The "symmetry-restoring interaction" includes the selfconsistent treatment of the Hamiltonian (2) as a special case. Using the notation (17)

$$\hat{H} = \hat{h} - \frac{\kappa_\circ}{2}\sum_{\mu=0,1\pm,2\pm} Q_\mu^2 \tag{20}$$

which in comparison to the one in Eq.(19) contains additionally the terms Q_0^2 and Q_{2+}^2 that are driving the beta-gamma vibrations. In this case one has to search for deformations $(\varepsilon, \gamma)_{sc}$ which comply with the selfconsistent conditions (cf. Eq. (4))

$$\frac{\kappa_\circ}{2} = \frac{1}{3}\frac{\hbar\omega_\circ\varepsilon}{\mathcal{Q}}\,, \qquad \sin\gamma = -\frac{\langle Q_{2+}\rangle}{\mathcal{Q}} = \sin\tilde{\gamma}. \tag{21}$$

According to Eq. (19) one recognizes that for the selfconsistent deformation $(\varepsilon, \gamma)_{sc}$ the common prefactor in the Hamiltonian (19) becomes equal to $\kappa_\circ/2$ and the three ratios of the Sin terms become one. Thus, for the sc deformations the Hamiltonian $\hat{H}$, Eq. (2) is fully rotational invariant, i.e. the commutator relations (15) are exactly satisfied.

At variance with the standard QQ-Hamiltonian (2), the coupling strengths of the three interaction terms $Q_{k\pm}^2$ in Eq. (19) are not equal for arbitrary choice of the deformation parameters (ε, γ). With the values of $\kappa_{1,2,3}$ obtained from Eq.(16) rotational symmetry is achieved *locally* because the commutator relations (15) are satisfied on average. This is in accordance with fact that the QRPA treats the wobbling motion as a small angle vibration. Local rotational invariance ensure that the spurious rotational excitations can be removed as the ones with the energies $E_{QRPA} = 0$ and $\hbar\omega$ (as in the sc case).

Below we present the results of a QRPA calculation with the Hamiltonian $\hat{H}$ of Eq.(19) using the deformation parameters (ε, γ) of Tab. II, which were found by a Nilsson-Strutinsky minimization [17]. Notice that γ is about° larger than the corresponding selfconsistent values.

Fig. 7 shows the calculated wobbling frequencies together with the experimental values. Compared to the

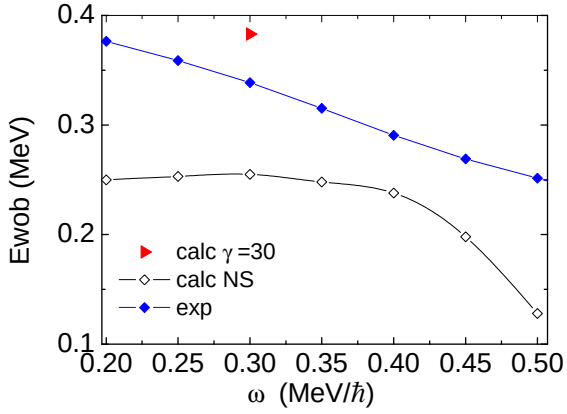

FIG. 7: (Color online) Wobbling frequencies in ^{163}Lu as a function of the rotational frequency. Experimental values (blue diamonds) are from [17]. The calculated values (solid line) are obtained with the Nilsson-Strutinsky (NS) deformations in table II. The single value (red triangle) is found for the deformation point ($\epsilon = 0.4, \gamma = 30$ deg).

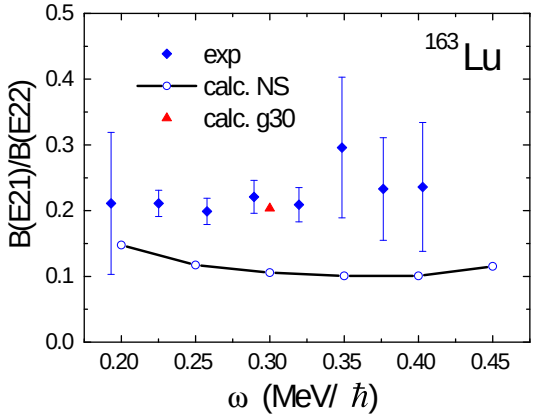

FIG. 8: (Color online) The ratios B(E21)/B(E22) between the inter and and intra band reduced transition probabilities B(E2, $I \to I-1)_{out}$/ B(E2, $I \to I-2)_{in}$ for the transitions between the TSD wobbling band and the TSD ground band in ^{163}Lu. Notations as in Fig. 7.

wobbling frequencies of the sc ISQQ model (cf. Fig. 4) the calculation with the Nilsson-Strutinsky deformations gives a flatter ω dependence, and the break down of the QRPA is slightly retarded. As seen in Fig. 15 of our study [5], the QRPA wobbling frequency curve resembles the one obtained by applying the HFA approximation to the Quasiparticle Triaxial Rotor QTR)description of transverse wobbling in ^{163}Lu using microscopic moments of inertia calculated by means of the TAC model. The HFA is a small-amplitude approximation like QRPA. The full quantal solution of the QTR shows a gradual decrease of the wobbling frequency with frequency, which is closer to experiment (cf. Fig. 15 of [5]).

Comparing Fig. 5 with Fig. 8. shows that the larger γ values lead to a 20 % increase of the ratio B(E2)$_{out}$/B(E2)$_{in}$. No reduction is obtained for the magnetic inter band transition strength as seen comparing Fig. 6 and Fig. 9. Hence with the larger γ values predicted by the Nilsson-Strutinsky calculation and the symmetry restoring QRPA we only accomplish a marginally better description of the TSD band properties.

We tried the case of maximal triaxiality $\gamma = 30°$ and $\varepsilon = 0.4$ for $\hbar\omega$=0.3 MeV. The results are included in Figs.(7-9). The wobbling frequency is enlarged, and even exceeds the experimental value. The ratio B(E2)$_{out}$/B(E2)$_{in}$ is about right, such that it could be adjusted by choosing an appropriate γ value between 25° and 30°. However, the small B(M1)$_{out}$ values remain unexplained. On the other hand, Ref. [13] demonstrated that QRPA based on the Woods-Saxon potential and the pertinent symmetry restoring interaction gives the experimental B(E2)$_{out}$/B(E2)$_{in}$ ratio for $\gamma \approx 20°$. In Ref. [14] the authors relate the small values of the ratio to artifacts of the Nilsson potential, which do not exist for the Woods-Saxon potential. In view of this, we attribute the

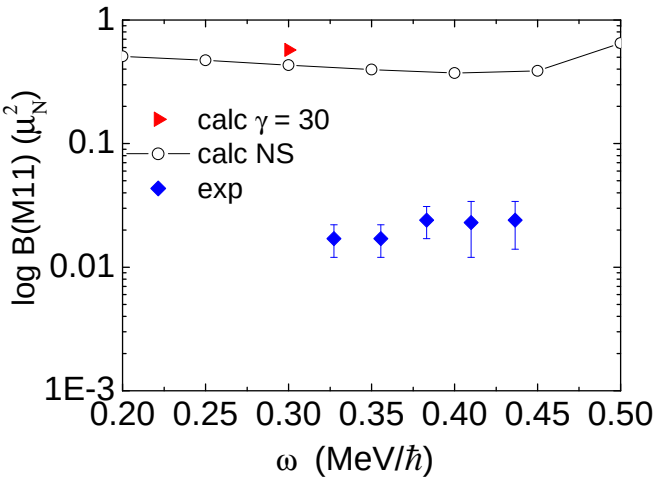

FIG. 9: (Color online) The reduced transition probabilities B(M11)= B(M1, $(I \to I-1))_{out}$ for the transitions between the TSD wobbling band to the TSD ground band in ^{163}Lu. Notations as in Fig. 7.

small ratio of B(E2)$_{out}$/B(E2)$_{in}$ obtained in our calculations to our choice of the Nilsson potential. Ref. [13] finds a comparable low wobbling frequency as we do and does not present the B(M1)$_{out}$ values. Thus, at this point we conclude the use of the isoscalar QQ residual interaction (including its symmetry restoring variants) only partly explains the experimental findings. This is the reason for study additional residual interactions in the following.

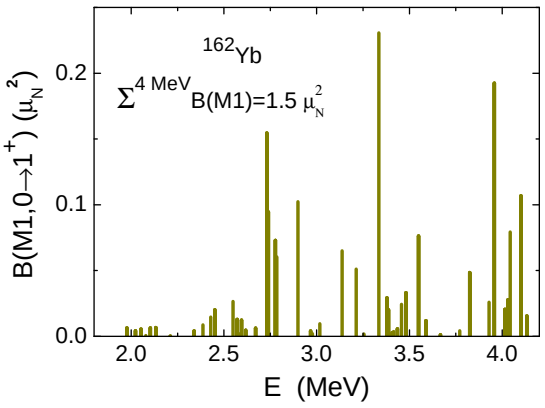

FIG. 10: (Color online) B(M1) distribution of ^{162}Yb obtained by rpa with the LL interaction, Eq. (23) choosing the strength constant $\kappa_{LL} = 0.5\,\mathrm{MeV}/\hbar^2$. The fragmented B(M1) strength adds up from 0 to 4 MeV to a sum strength of 1.5 μ_N^2 that can be interpreted as scissors strength.

III. ADDITIONAL RESIDUAL INTERACTION TERMS

The experimental fact that the inter band M1 transitions of the wobbling mode are strongly suppressed in comparison to the inter band E2 transitions is a major motivation to study further interaction terms aside the QQ interaction considered so far. It is the question, what makes that the magnetic de-excitation so small. It is known that the scissors mode collects the low-lying M1 strength which is concentrated higher up in the energy region of 3-4 MeV [22]. A possible mechanism for suppressing the M1 strength of low-energy states is shifting it to the scissors mode, like the electric dipole strength of low energy states is shifted to the Giant Dipole Resonance.

Before presenting the results of our QRPA calculations with additional interaction terms a note about the removal the spurious rotational modes is in order. When adding interaction terms the strength constants of which are not fixed by selfconsistency or rotational invariance the rotational modes shift away from their true energies $E_{QRPA} = 0$, $\hbar\omega$ and mix with the wobbling mode, such that the results are distorted by spurious effects. Therefore we apply the method proposed in Ref. [24] to eliminate the spurious modes. The QRPA Hamiltonian is complemented by the IS term $\kappa_j \mathbf{J}\cdot\mathbf{J}$ which acts like a spring force for the unwanted angle vibrations of the total angular momentum $\mathbf{J}$ in the rotating system. Choosing the stiffness parameter large, as $\kappa_j \geq 10^2$, the excitation energies for the rotational spurious states are shifted far outside the considered energy range, which prevents them from mixing with the physical modes.

Our first modification was motivated by the purely collective picture of the scissors mode being an angle vibration of the proton system against the neutron system with an IV QQ restoring force [23]. Accordingly, we added to the ISQQ Hamiltonian (2) an IV QQ interaction term built from the operators $\hat{Q}^{iv}_m = \hat{Q}_m(\pi)$ - $\hat{Q}_m(\nu)$. Knowing the selfconsistent strength $\kappa_\circ$ from table I we set the isovector strength $\kappa^{iv}_\circ = r\,\kappa_\circ$ where the value of the ratio r was varied in the range -1.5 to - 3.5 [1]. This addition lead to only a minor change of the B(E2/M1) transition probabilities. However, it increased the wobbling frequency, such that the experimental wobbling frequencies could be fitted by choosing an appropriate value of r.

Second, we considered the spin-spin (SS) interaction, because it has been successfully applied in connection with the scissors mode to explain the systematic accumulation of 1^+ states between 3-5 MeV with considerable M1 decay strengths [20]. We included both the IS and the isovector (IV) spin-spin interactions defined by

$$\begin{aligned} V_{LL}^{(is,iv)} &= \sum_{m=-1,1} (-1)^m\, \hat{S}^{(is,iv)}_{m}\, \hat{S}^{(is,iv)}_{-m}, \\ \hat{S}^{(is,iv)}_{m} &= \hat{S}_m(\tau=+1) \pm \hat{S}_m(\tau=-1). \end{aligned} \qquad (22)$$

We determined the SS strength parameters by extrapolating the A-dependent strength parameters given in the work of De Coster and Heyde [26] used there for QRPA calculations of the 1^+. The SS interactions are then added to the selfconsistent ISQQ Hamiltonian (2) described in Sec. II A. The results of the QRPA calculation for the frequency $\hbar\omega = 0.3$ MeV/$\hbar$ can be summarized as follows: The IS and IV SS terms have only negligible effects on both the wobbling energy and the B(E2/M1) transition probabilities. The lowering of the $\mathrm{B(M1)}_{out}$ value is small, i.e. there is not much shift the M1 strength into the scissor region.

Our third modification was motivated by the interpretation that the scissors mode represents an angle vibration of the orbital a.m. vector $\vec{\mathbf{L}}_\pi$ of the protons versus the orbital a.m. vector $\vec{\mathbf{L}}_\nu$ of the neutrons. Accordingly, we complemented the ISQQ Hamiltonian (2) by an interaction term that is composed of the isovector orbital angular momenta:

$$V_{LL} = \kappa_{LL}(\vec{\mathbf{L}}_\pi - \vec{\mathbf{L}}_\nu)^2. \qquad (23)$$

Ref. [27] successfully used an interaction of the type $V_{JJ} = \kappa_{JJ}(\vec{\mathbf{J}}_\pi - \vec{\mathbf{J}}_\nu)^2$ to describe the M1 strength in the scissors region of the Mo isotopes. We checked that such IV JJ interaction gives nearly the same results as the LL interaction when the coupling constant is appropriately chosen.

The effects of adding the LL interaction are shown in Figs.(11- 13). The calculated wobbling energy increases due to the repulsive LL term. We find a good match to the experimental curve when choosing the strength constant $\kappa_{LL} = 0.5$ MeV/$\hbar^2$. The inter band E2 transitions stay almost unchanged, which is expected from a current-current interaction. The same value of κ_{LL} gives

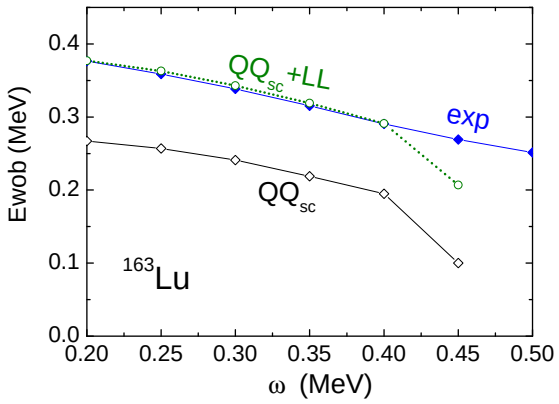

FIG. 11: (Color online) Wobbling frequencies in ^{163}Lu as a function of the rotational frequency. Experimental values (blue diamonds) are from [17]. Calculated values are obtained with QRPA using (solid line) selfconsistent ISQQ interaction and (green dotted line) additionally LL interaction (see Eq. (23))

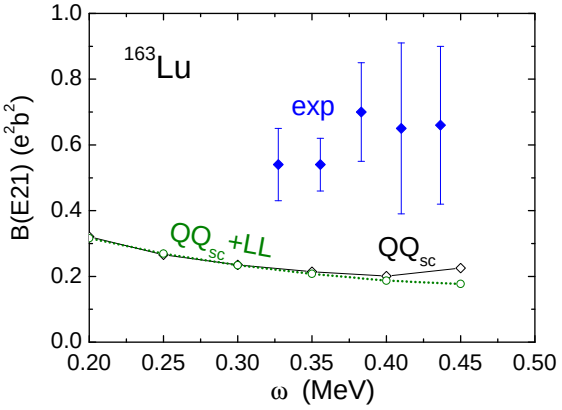

FIG. 12: (Color online) The reduced transition probabilities B(E21)=B(E2, $I \to I-1)_{out}$ for the transitions between the TSD wobbling band and the TSD ground band in ^{163}Lu. Calculated values are obtained with QRPA using (solid line) selfconsistent ISQQ interaction and (green dotted line) additionally LL interaction (see Eq. (23)).

the desired suppression of the B(M1) transition strength, which comes close to the measured values.

Hence, the QRPA with additional LL interaction is capable of providing a satisfactory description of the wobbling frequencies and of the magnetic properties. This raises the question whether the adjusted coupling parameter κ_{LL} is consistent with the experimental information about the scissors mode built on the ground states of the even-even neighbors. We calculated the distribution of B(M1, $0 \to 1^+$) from the ground state of ^{162}Yb using the same QRPA approach as for the wobbling mode in ^{163}Lu. The deformation $\beta = 0.225$ from was taken Ref. [25], and the value $\kappa_{LL} = 0.5\,\mathrm{MeV}/\hbar^2$ used for the LL interaction. The resulting distribution is shown in Fig. 10 for interval E=2-4 MeV, which is the suggested region of the scissors mode. There is no experimental information for the unstable nuclid ^{162}Yb about the distribution of 1^+ states to compare with. However, the systematics of the summed B(M1) strength presented in Refs. [21, 22] provides a clue concerning the coupling constant. Our value $\kappa_{LL} = 0.5\,\mathrm{MeV}/\hbar^2$ gives a summed strength $\Sigma B(M1) \approx 1.5\,\mu_N^2$ for the 1^+ excitations between 0-4 MeV, which agrees with the value from the systematics for the deformation $\beta = 0.225$ of ^{162}Yb. The agreement indicates that the coupling of the transverse wobbling to the scissors mode at high spin and the M1 strength of the low-spin scissors mode can be accounted for by one and the same value of κ_{LL}.

The improvements achieved by including the IV LL interaction term can be taken as an indication that the wobbling motion is not a pure orientation vibration of the quadrupole mass tensor with respect to the angular momentum vector. It implies a coupling to vibrations of the proton and neutron currents against each other (see the interpretation of the scissors mode in Ref. [28]).

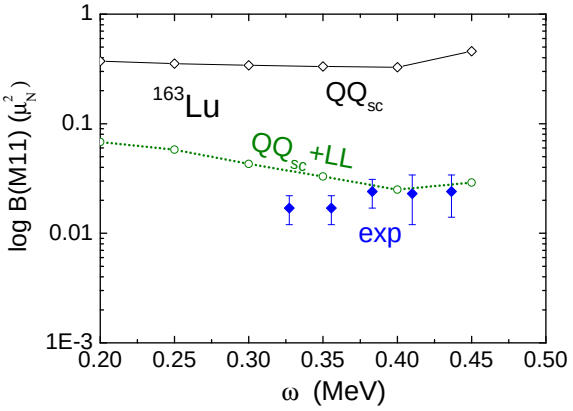

FIG. 13: (Color online) The reduced transition probabilities B(M11)= B(M1, $(I \to I-1))_{out}$ for the transitions between the TSD wobbling band to the TSD ground band in ^{163}Lu. Calculated values are obtained with QRPA using (blue line) selfconsistent ISQQ interaction and (green dotted line) additionally LL interaction (see Eq. (23)).

The microscopical origin of such schematic interaction of the current-current type remains obscure at this point. However, it is noted that Ref. [20] well describe the low-spin scissors mode in the framework of QRPA based on a symmetry restoring interaction that is derived from a deformed Woods-Saxon potential. The pertinent commutators with the deformed spin-orbit potential will generate IV terms of containing the the momentum and spin operators, which may be schematically accounted for by the LL interaction. It would be interesting to see how QRPA based on the symmetry restoring interaction of Ref. [20] describes transverse wobbling.

IV. SUMMARY AND CONCLUSIONS

The transverse wobbling mode in ^{163}Lu has been reinvestigated in the frame work of Quasiparticle Random Phase Approximation. The QRPA calculations were based on the rotating mean field that consisted of a deformed Nilsson potential and an attenuated monopole pair field. Various versions of the residual interaction were investigated. For all variants studied, The QRPA wobbling frequencies decrease with the rotational frequency, so confirming the transfers character of the solution. The results obtained with an isoscalar Quadrupole-Quadrupole interaction and selfconsistent deformation parameters in essence agree with previous QRPA calculations [11], which used the same mean field Hamiltonian but another way of finding the solutions. The calculated wobbling frequencies show the right descent with the rotational frequency but are only 60% of the experimental excitation energy. The $B(E2)_{out}/B(E2)_{in}$ ratios for the inter band transitions connecting the wobbling with the ground band and the intra band transitions show the characteristic collective enhancement, but are low by about a factor two. The $B(M1)_{out}$ values of these inter band transitions are a factor 10 too large compared with experiment.

To check whether the small selfconsistent values of the triaxiality parameter $\gamma \approx 10^\circ$ are the cause for the deviations, we tried the QRPA variant based on a factorized residual interaction that is derived from the mean field by requiring local rotational invariance, which allows one to chose freely the deformation parameters. Using $\gamma \approx 20^\circ$, which is the equilibrium value of the Nilsson-Strutinsky Routhian, slightly moves the results toward the experimental values, however the discrepancies remain as substantial as before. Increasing the triaxiality to $\gamma \approx 30^\circ$ brings the $B(E2)_{out}/B(E2)_{in}$ ratio up to the experimental value and the wobbling frequency a bit above the experimental one, such that γ values somewhat below 30° will lead to a match with experiment. However, we do not favor this possibility for the following reasons. Cranked mean field calculations generally predict smaller triaxiality of $\gamma \approx 20^\circ$. Ref. [13] demonstrated that using a Woods-Saxon potential with $\gamma \approx 20^\circ$ gives the experimental $B(E2)_{out}/B(E2)_{in}$ ratios. As discussed next, $\gamma \approx 30^\circ$ would shift the wobbling frequencies too high when the additional residual LL interaction is taken into account. Rather we share the view of Ref. [14] that the low $B(E2)_{out}/B(E2)_{in}$ ratios are an artifact of the Nilsson potential, which will be removed by replacing it by a more realistic potential.

Our study confirms previous findings that QRPA based on an isoscalar QQ-type interaction gives too small wobbling frequencies and too large inter band B(M1) values. These discrepancies are removed by including a repulsive isovector current-current interaction of the schematic form $\kappa_{LL}(\vec{\mathbf{L}}_\pi - \vec{\mathbf{L}}_\nu)^2$, where $\vec{\mathbf{L}}$ is the total orbital angular momentum. This LL interaction couples the wobbling mode to the scissors mode, which represents a concentration of orbital M1 strength in the region E=3-4 MeV above the yrast line. The $B(M1)_{out}$ values are reduced, because M1 strength is shifted into the scissors region, and the wobbling frequencies increase because the LL interaction is repulsive. The same interaction strength κ_{LL} generates the right upshift of the wobbling frequencies and the right suppression of the $B(M1)_{out}$ values toward the experimental values. Moreover, using the same κ_{LL} value, QRPA on the ground state of the neighbor ^{162}Yb reproduces the cumulative M1 strength below 4 MeV, known from experimental systematics.

Altogether, QRPA based on the combination of the isoscalar QQ and isovector LL interaction well reproduces the experiments on transverse wobbling of the triaxial strongly deformed nuclide ^{163}Lu. The mode represents mainly an oscillation of the triaxial charge distribution relative to the angular momentum vector, which is manifest by strong E2 transitions from the one-phonon to the zero-phonon wobbling bands. Additionally, it contains a substantial admixture of scissors-like oscillations of the proton currents against the neutron currents, which increase the wobbling frequency and reduce the M1 transition strength between the wobbling bands by a factor of 10. In the other case of a well studied example of transverse wobbling, ^{135}Pr, the QTR calculations in Ref. [6], which do not take into account the coupling to the scissors mode, overestimate the $B(M1)_{out}$ values by a factor of three. One expects a weaker coupling to the scissors mode, because ^{135}Pr is much less deformed than ^{163}Lu and it is known that the M1 strength collected by the scissors mode increases quadratically with the deformation parameter [21, 22].

Ref. [29] reported a suppression of the $B(M1)_{out}$ between rotational bands built on different members of the quasineutron $j_{15/2}$ multiplet in ^{235}U by a factor of 20-50 compared to estimates in the framework of the Quasiparticle - Rotor model. In addition, the authors tabulated examples of $B(M1)_{out}$ values between bands of high-j multiplet members, which all appear strongly suppressed. This systematic quenching of M1 strength suggests that the scissors mode draws M1 strength from the low-energy transitions in analogy to the quenching of the low-energy E1 transitions by coupling to the GDR (screening).

Support by the US Department of Energy Grant No. DE-FG02-95ER40934 is acknowledged. Unfortunately Fritz Dönau passed away before completion of this work. Our community lost a great scientist, an enthusiastic researcher, and a friend whom many of us will miss.

[1] A. Bohr and B. R. Mottelson, *Nuclear Structure*, Vol. II (Benjamin, New York), 1975.

[2] S. W. Ødegård *et al.*, Phys. Rev. Lett. **86**, 5866 (2001).

[3] H. J. Jensen *et al.*, Nucl. Phys. A **695**, 3 (2001).
[4] D. R. Jensen *et al.*, Nucl. Phys. A **703**, 3 (2002).
[5] S. Frauendorf and F. Dönau, Phys. Rev. C **89**, 89, 014322 (2014)
[6] J. T. Matta *et al.* Phys. Rev. Lett. **114**, 082501 (2015)
[7] I Hamamoto, Phys. Rev. C **65**, 044305 (2002).
[8] I. Hamamoto and G. B. Hagemann, Phys. Rev. C **67**, 014319 (2003).
[9] K. Sugawara-Tanabe and K. Tanabe, Phys. Rev. C **82**, 051303 (2010).
[10] Y. R. Shimizu, and M. Matsuzaki, Nucl. Phys.**A588**, 559 (1995)
[11] M. Matsuzaki, Y. R. Shimizu, and K. Matsuyanagi, Phys. Rev. C **65**, 041303(R) (2002).
[12] M. Matsuzaki and S.-I. Ohtsubo, Phys. Rev. C **69**, 064317 (2004)
[13] T. Shoji and Y. R. Shimizu, Int. Jour. Mod. Phys. E **15** 1407 (2006)
[14] Y. R. Shimizu, T. Shoji and M. Matsuzaki , Phys. Rev. C **77**, 02439 (2008).
[15] D. Almehed, F. Dönau and S. Frauendorf, Phys. Rev. C **83** 054308 (2011)
[16] S. Frauendorf, Nucl. Phys. **A677**, 115 (2000)
[17] A. Görgen *et al.*, Phys. Rev. C **69**, 031301(R) (2004).
[18] P. Ring and P. Schuck, *The Nuclear Many-Body Problem*, (Springer, New York, 1980)
[19] M.I. Baznat and N.I. Pjatov, Sov.J.Nucl.Phys. **21**, 365 (1975)
[20] R. Nojarov and A. Faessler, Nucl. Phys. **A484** 1 (1988)
[21] W. Ziegler, C. Rangacharyulu, A. Richter, and C. Spieler, Phys. Rev. Lett. **65**, 2515 (1990)
[22] K. Heyde, P. von Neumann-Cosel, A. Richter, Rev. Mod. Phys.**82**, 2365
[23] Lo Iudice, N., and F. Palumbo, Phys. Rev. Lett. **41**, 1532
[24] F. Dönau, Phys. Rev. Lett. 94, 092503 (2005).
[25] P. Möller, J.R. Nix, W.D. Myers and W.J. Swiatecki, Atomic Data and Nuclear Data Tables **59**, 185-381
[26] C. DeCoster, K. Heyde, Nucl. Phys. A**529** , 507 (1991).
[27] G. Rusev *et al.*, Phys. Rev. C **73**, 044308 (2006)
[28] I. Hamamoto and S. Aberg, Phys. Lett. B **145**, 163 (1984)
[29] D. Ward *et al.* Phys. Rev. C **86**, 064319 (2012)